Supporting Information

A straightforward approach to improve NCM523/Graphite pouch batteries performance in wide temperature range at 4.35 V by film-forming additive *N*-Phenylimidodisulfuryl fluoride (PhFSI)

Guoliang Yang, [a] Zhaohao Huang, [a] Irfan Majeed, [a] Chaojun Fan, [b] Jiasheng Lu, [b] Kai Wang, [b] Weizhen Fan, [b*] Jingwei Zhao, [b*] Zhuo Zeng [a*]

[a] School of Chemistry, South China Normal University, Guangzhou 510006, Guangdong, China

Email: zhuoz@scnu.edu.cn

[b] Guangzhou Tinci Materials Technology Co., Ltd., Guangzhou 510760, Guangdong, China

Email: fanweizhen@tinci.com, zhaojingwei@tinci.com

Table of Contents

Synthesis of PhFSI and the structural identification of the PhFSI

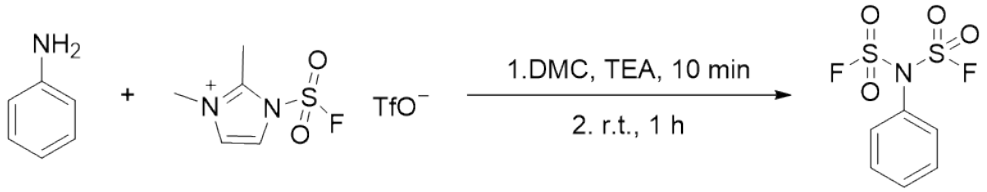

The (fluorosulfonyl)(phenyl)sulfamoyl fluoride (PhFSI) was synthesized basically according to Dong's method [1]. We substituted the acetonitrile to DMC which is a green solvent and also a part of electrolytes. To a solution of aniline in DMC stirred at 0 °C, 1-(fluorosulfonyl)-2,3-dimethyl-1H-imidazol-3-ium trifluoromethanesulfonate was added directly and the solution became faint yellow with insoluble floating salts. After stirring for 10 minutes, triethylamine was added slowly drop by drop to trigger the reaction as shown by gradually dissolved salts and deeper yellow color. Then the reaction system was transferred to room temperature and stirred for 1 hour to finish reaction. The mixture was extracted with water for 3 times and aqueous layer was extracted for 1 time. The combined organic layer was dried with anhydrous sodium sulfate and the purification were achieved through silica gel chromatography to afford PhFSI as colorless crystals (yield: 80%), R_f (hexane) 0.8. The molecular structure of PhFSI was identified by ^{1}H, ^{13}C and ^{19}F NMR spectrum using ACN-*d*3 as solvent and the purity was 99.98% measured by gas chromatography (GC, Agilent 7890A).

The ^{1}H NMR spectrum of the PhFSI

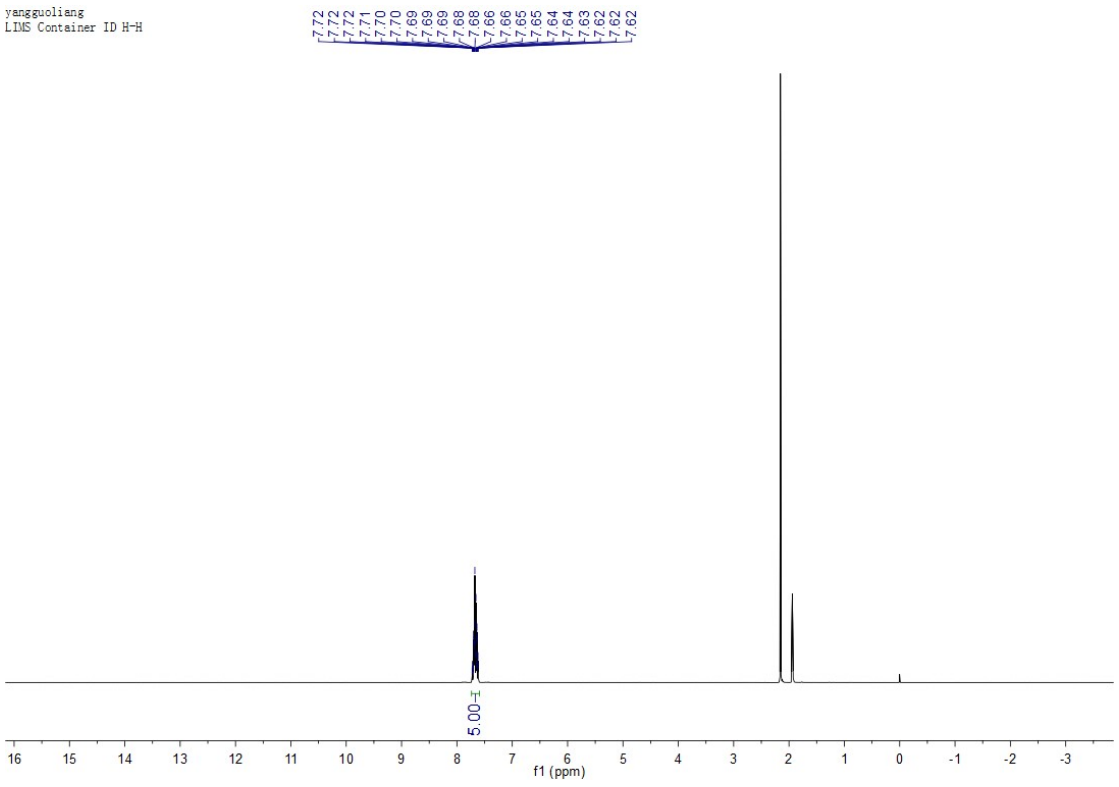

^{1}H NMR (400 MHz, CD_3CN) δ 7.72-7.62 (m, 5 H)

The ^{13}C NMR spectrum of the PhFSI

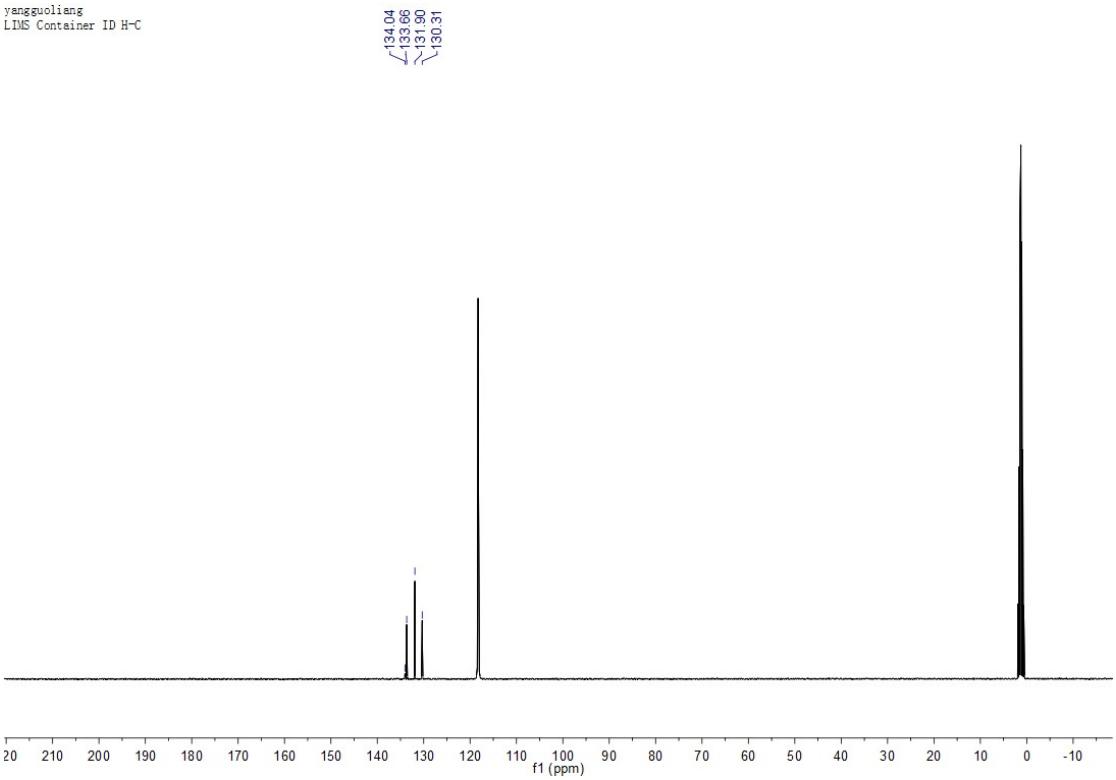

^{13}C NMR (101 MHz, CD_3CN) δ 134.02 (s), 133.66 (s), 131.90 (s), 130.31 (s).

The ^{19}F NMR spectrum of the PhFSI

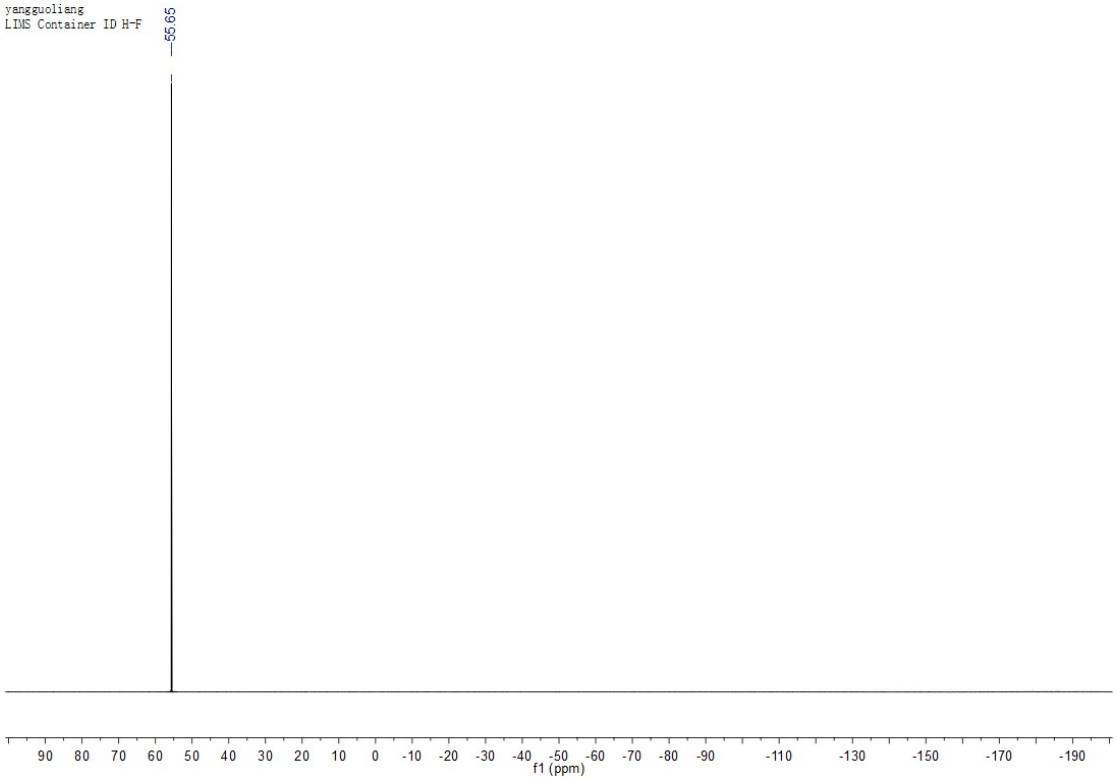

^{19}F NMR (376 MHz, CD_3CN) δ 55.65 (s).

Gas chromatography (GC) analysis results of the *N*-Phenylimidodisulfuryl fluoride

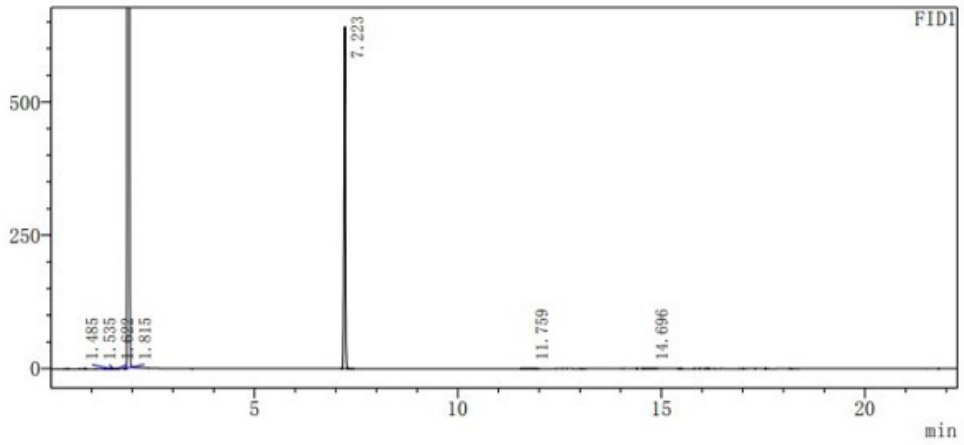

FID1

Peak	Retention Time	Compound	Height	Area	Area%
1	1.485		82	98	0.007
2	1.535		154	230	0.016
3	1.622		120	145	0.010
4	1.815		710	853	0.059
5	7.223		641541	1441499	99.791
6	11.759		79	949	0.066
7	14.696		71	748	0.052
			642757	1444521	100.000

Fitting values of the EIS spectra of the NCM523/Graphite cells

Samples	Blank	PhFSI	Blank	PhFSI	Blank	PhFSI
R (mΩ)	1st		200th		500th	
R_b	38.86	36.93	42.07	37.23	69.09	46.75
R_f	8.10	7.58	4.98	5.05	17.38	5.45
R_{ct}	14.02	10.15	31.25	17.62	87.22	65.72

Tab. S1 The fitted R_b, R_f and R_{ct} value at 1st, 200th and 500th cycle of NCM523/Graphite pouch cells cycled at 1 C at 25 °C.

Samples	Blank	PhFSI	Blank	PhFSI
R (mΩ)	1st		400th	
R_b	39.73	37.12	81.69	46.73
R_f	8.25	7.43	22.8	9.54
R_{ct}	14.13	10.32	57.82	39.68

Tab. S2 The fitted R_b, R_f and R_{ct} value at 1st and 400th cycle of NCM523/Graphite pouch cells cycled at 1 C at 45 °C.

Cycling performances of NCM523/Graphite cells with various concentrations of PhFSI and the EIS spectra before cycling

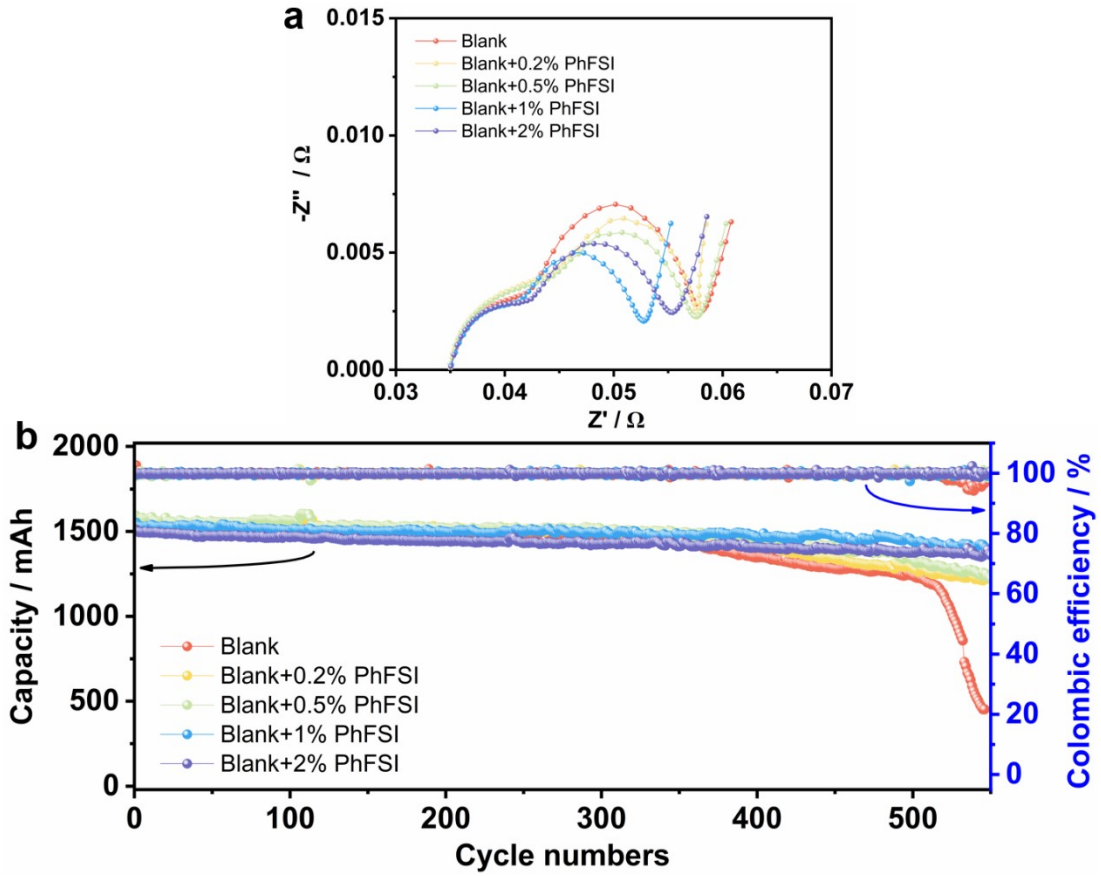

Fig. S1 (a) The EIS spectra of the NCM523/Graphite pouch cells with the Blank and different concentrations of PhFSI before cycling and (b) their cycling performances at 1 C at 25 °C.

Supplement data for NCM523/Graphite cells cycling at 45 ºC.

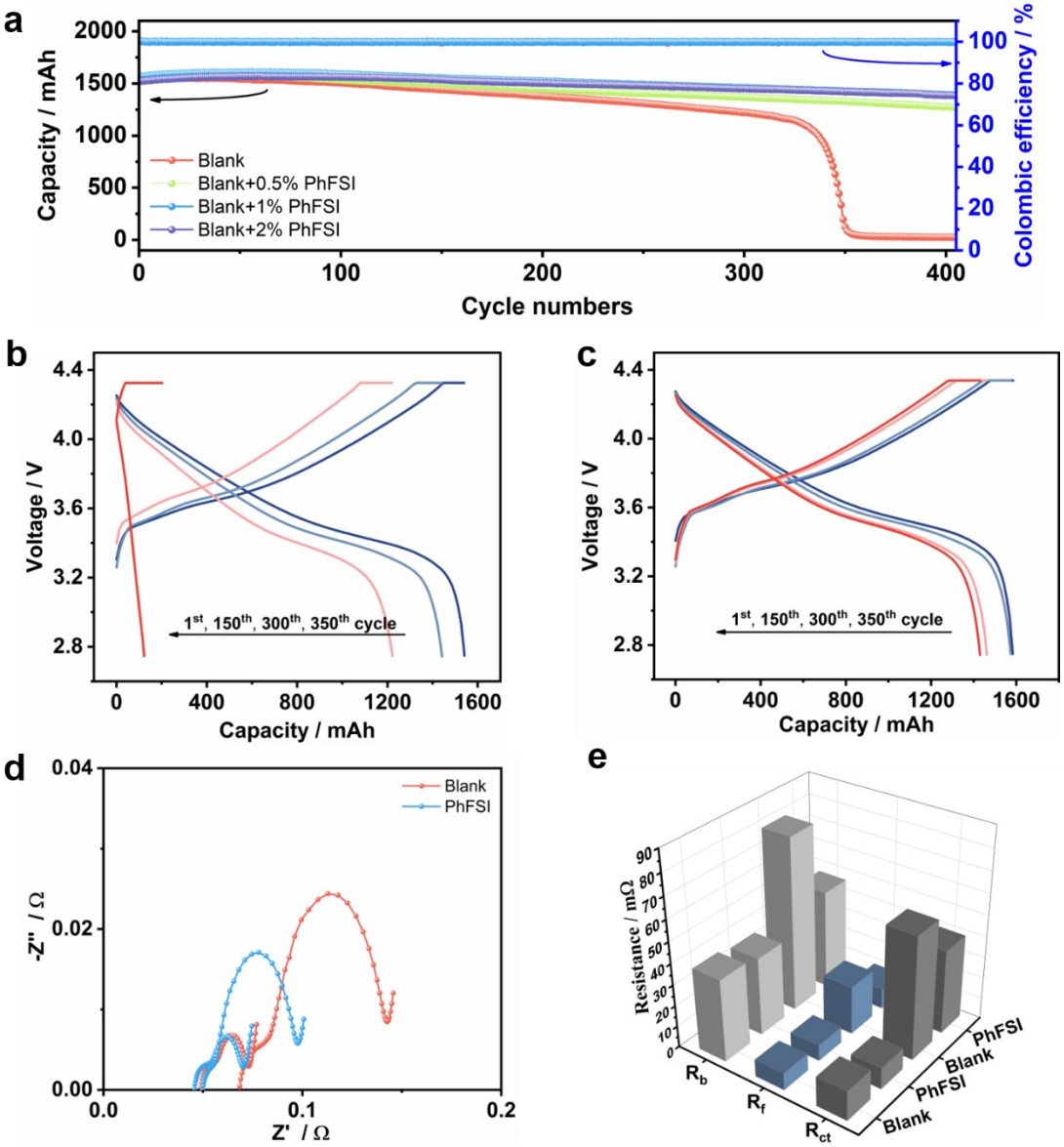

Fig. S2 (a) The cycling performances of NCM523/Graphite with/without PhFSI at 1 C under 45 °C. The charge-discharge curves of the batteries (b) with the Blank and (c) 1% PhFSI at 1st, 150th, 300th, 350th cycle. (d) The EIS spectra before and after cycling at 45 °C and (e) corresponding fitted R_b, R_f, R_{ct} values.

Performances of NCM523/Graphite pouch cells with/without PhFSI storing at 60 °C for 7 days

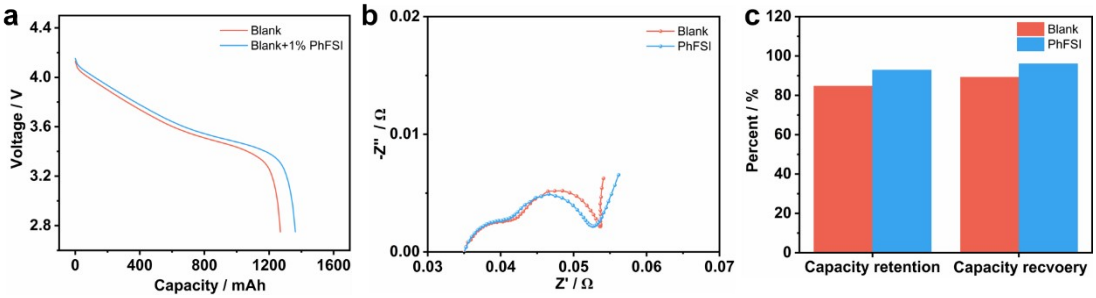

Fig. S3 The (a) discharge curves, (b) EIS spectra and (c) relevant capacity retention/recovery of the NCM523/Graphite pouch cells with/without PhFSI after storing at 60 °C for 7 days.

Supplement data for NCM523/Graphite cells cycling at -20 °C.

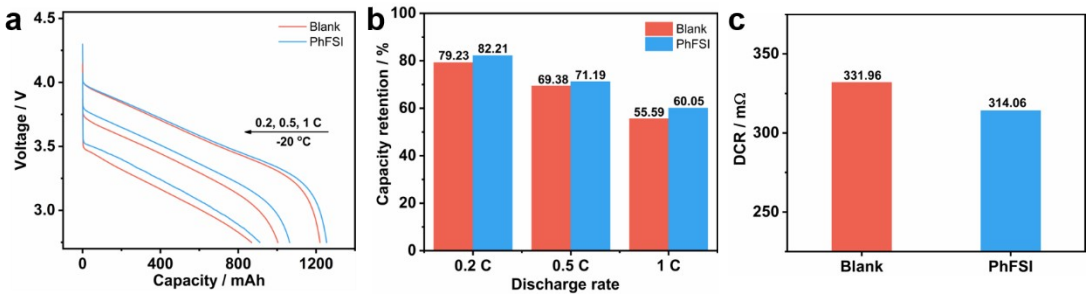

Fig. S4 (a) The discharge curves of NCM523/Graphite with/without PhFSI discharged at 0.2, 0.5, and 1 C under -20 °C. (b) The capacity retention of batteries discharged at -20 °C. (c) DCR values measured at -20 °C.

Cycling performances of NCM811/Graphite cells with/without PhFSI and the EIS spectra during cycling

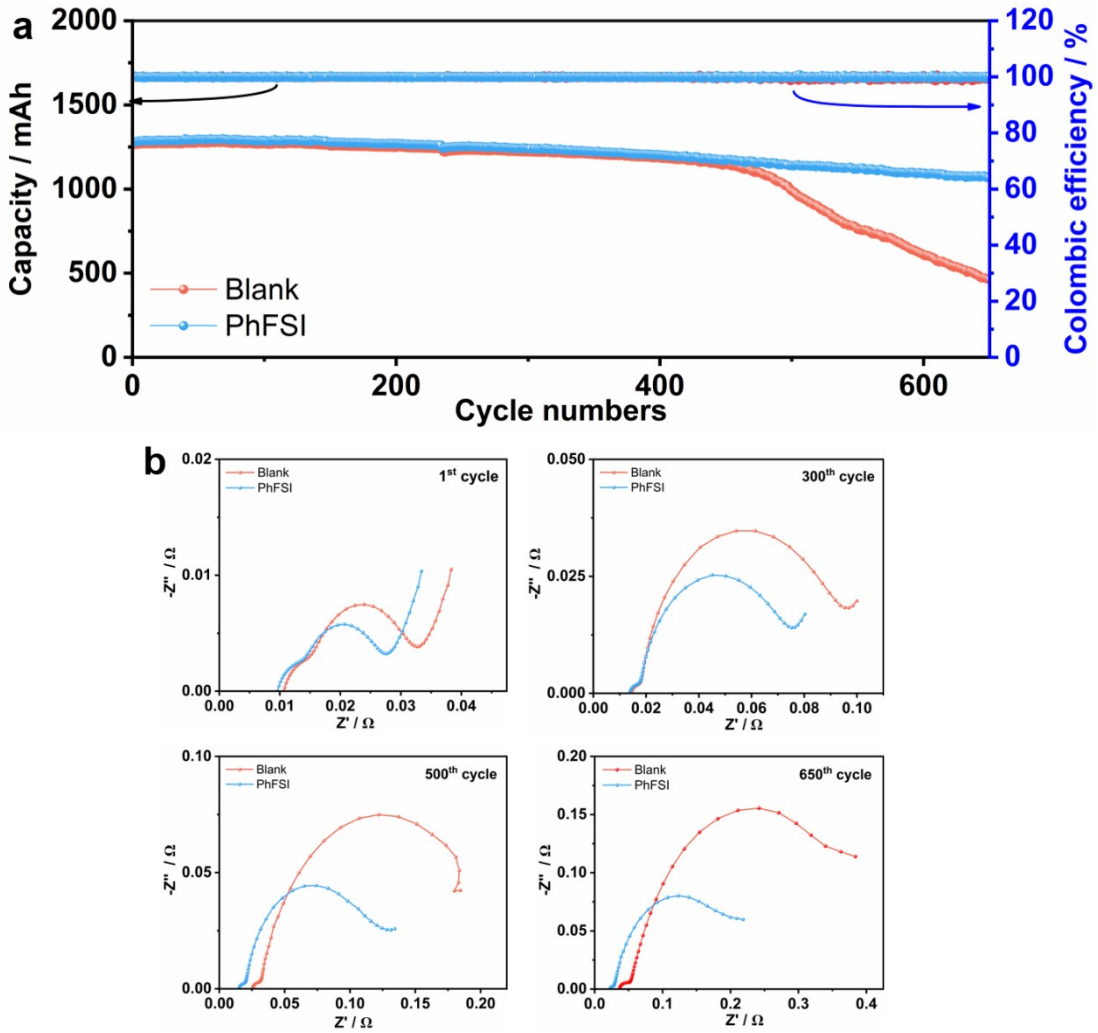

Fig. S5 (a) The cycling performances and (b) the EIS spectra of the NCM811/Graphite pouch cells with/without 1% PhFSI cycling at 1 C at 25 °C.

Pictures of the cathodes and anodes before and after cycling at 25 °C

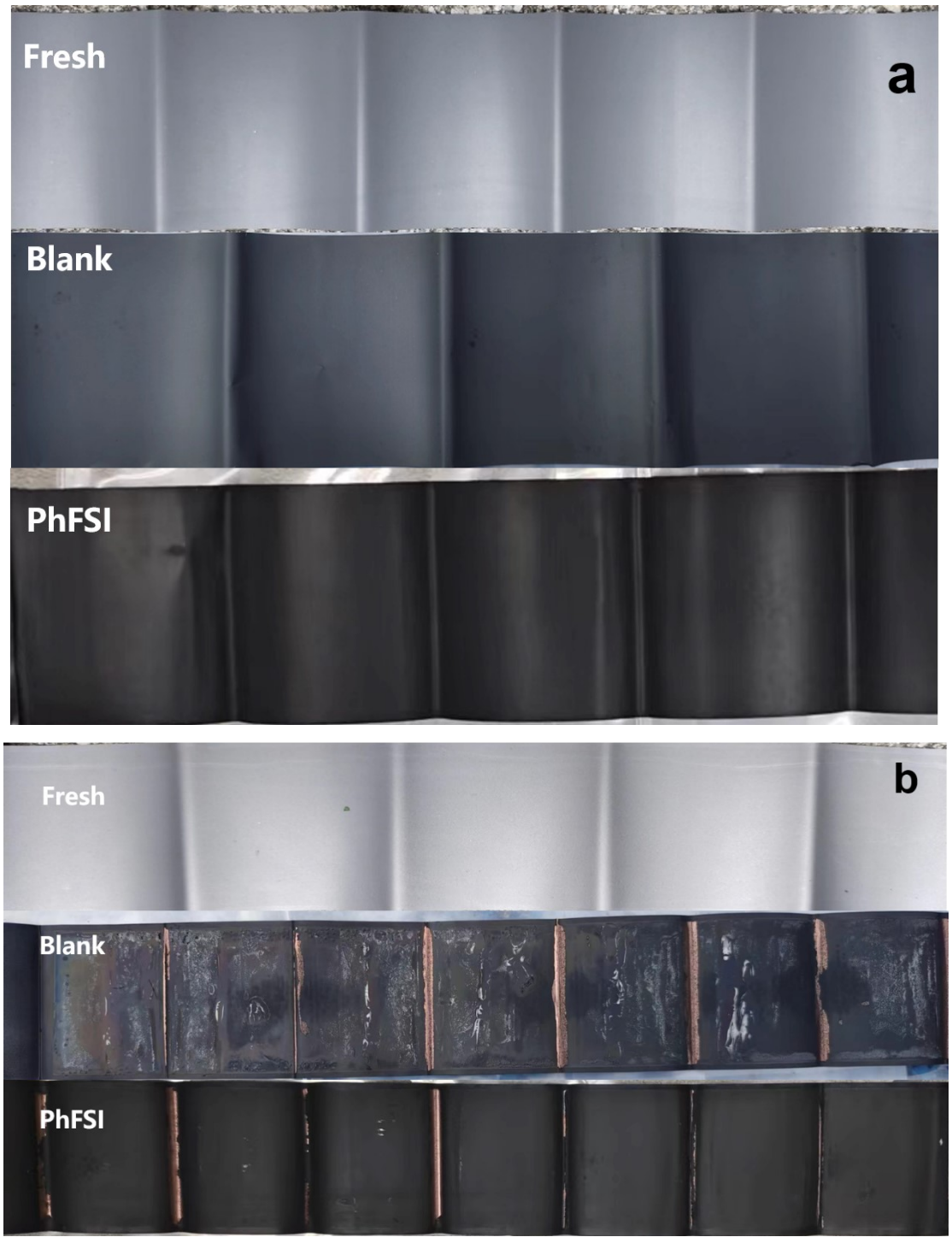

Fig. S6 Pictures of (a) the NCM523 cathode and (b) the graphite anode of the pristine, cycled with the Blank and PhFSI.

Cross-sectional image of the NCM523 in the blank and raman results of the coverage on the anode with the Blank

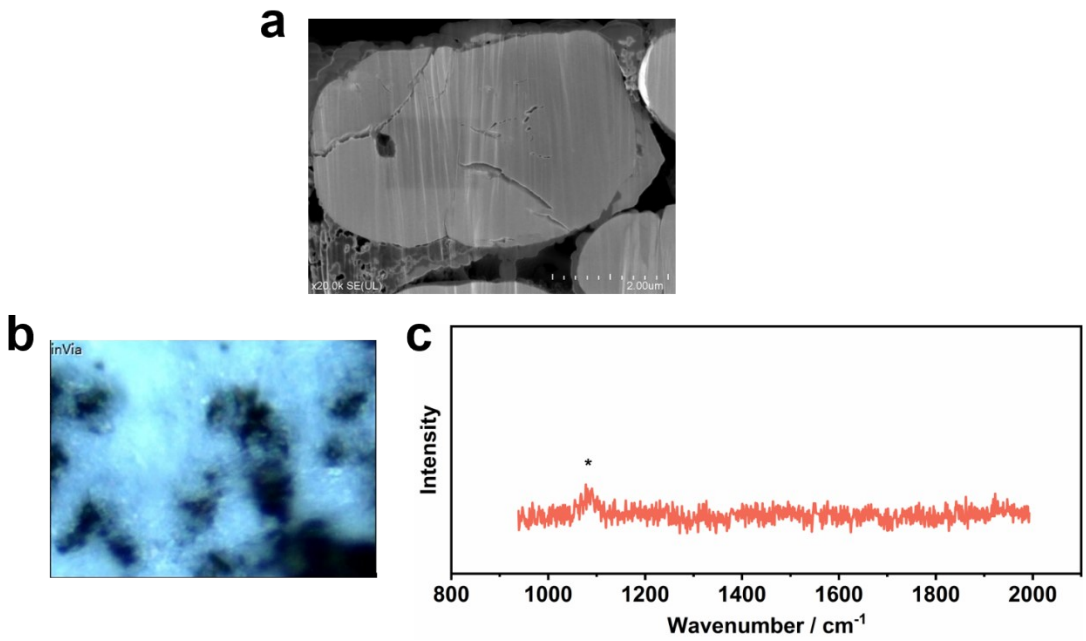

Fig. S7 (a) The anode observation of the Blank under confocal micro-raman spectrometer and (b) the corresponding results. (c) The cross-sectional image of the Blank NCM523.

XPS spectra of the Ni and Mn analysis on the cathodes and anodes with/without PhFSI.

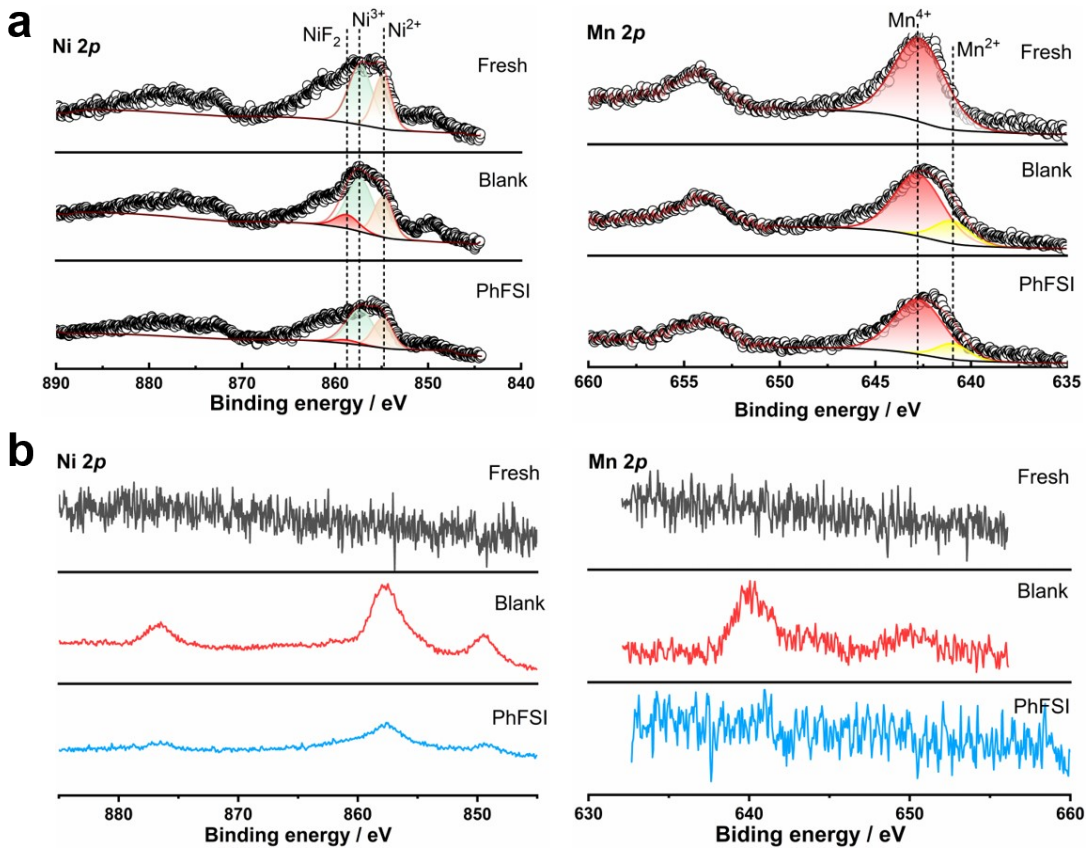

Fig. S8 The XPS spectra of the Ni 2*p* and Mn 2*p* of the (a) NCM523 cathodes and (b) Graphite anodes.

Contact angles and viscosity of the electrolyte with/without PhFSI.

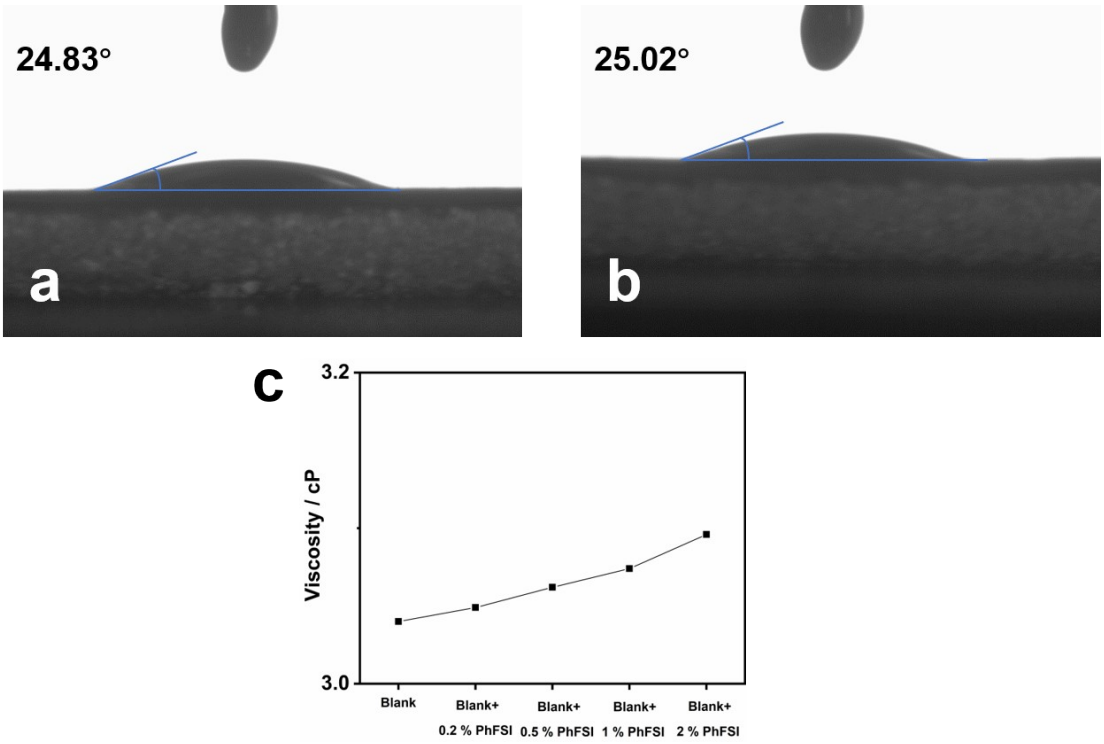

Fig. S9 The contact angles of the electrolyte (a) without (b) with 1% PhFSI measured at 25 °C and (c) vicosity of electrolytes with/without PhFSI at 25 °C.

Calculations of AIE and EA energies as well as binding energy between Li+ and electrolyte components.

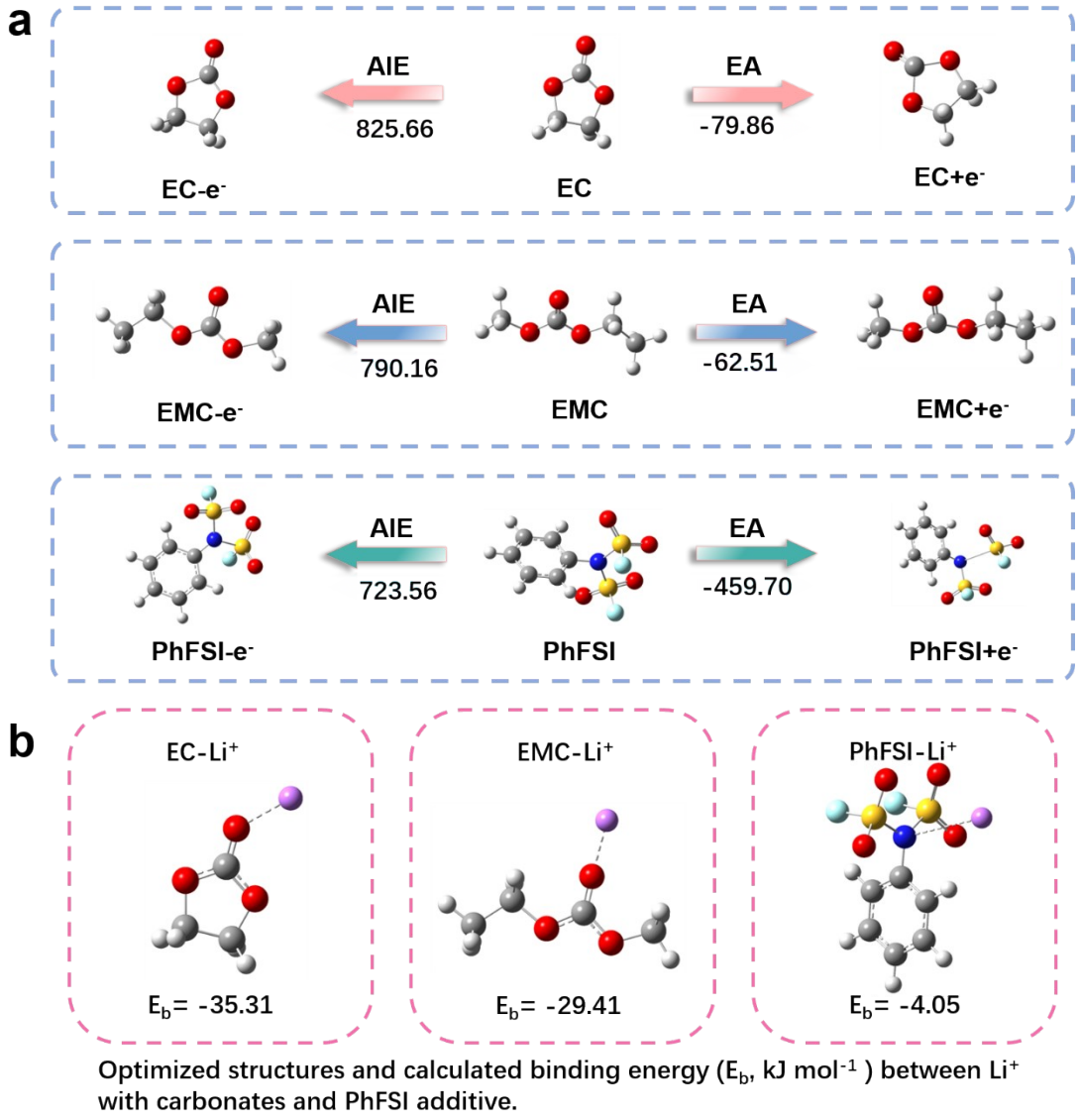

Fig. S10 The optimized structures of the EC, EMC and PhFSI in neutral, obtaining and losing one electron state with resultant AIE, EA as well as (c) the biding energy of electrolyte components with Li^+ (kJ mol^{-1}).

As seen in the Fig. S10a, PhFSI exhibited lowest AIE and EA compared to EC and EMC, indicating PhFSI is easier to lose/receive electron and decompose preferentially. Moreover, the negative binding energiy between PhFSI and Li+ is lower than those of with carbonates, i.e. PhFSI-Li^+ -4.05 KJ mol^{-1}, EMC-Li^+ -29.41 KJ mol^{-1}, EC-Li^+ -35.31 KJ mol^{-1}. Therefore, PhFSI is poor to coordinate in the inner Li^+ solvation sheath. indicating that PhFSI is more prone to decompose on the electrode as well.[2]

CV spectra of the NCM/Li and Graphite/Li

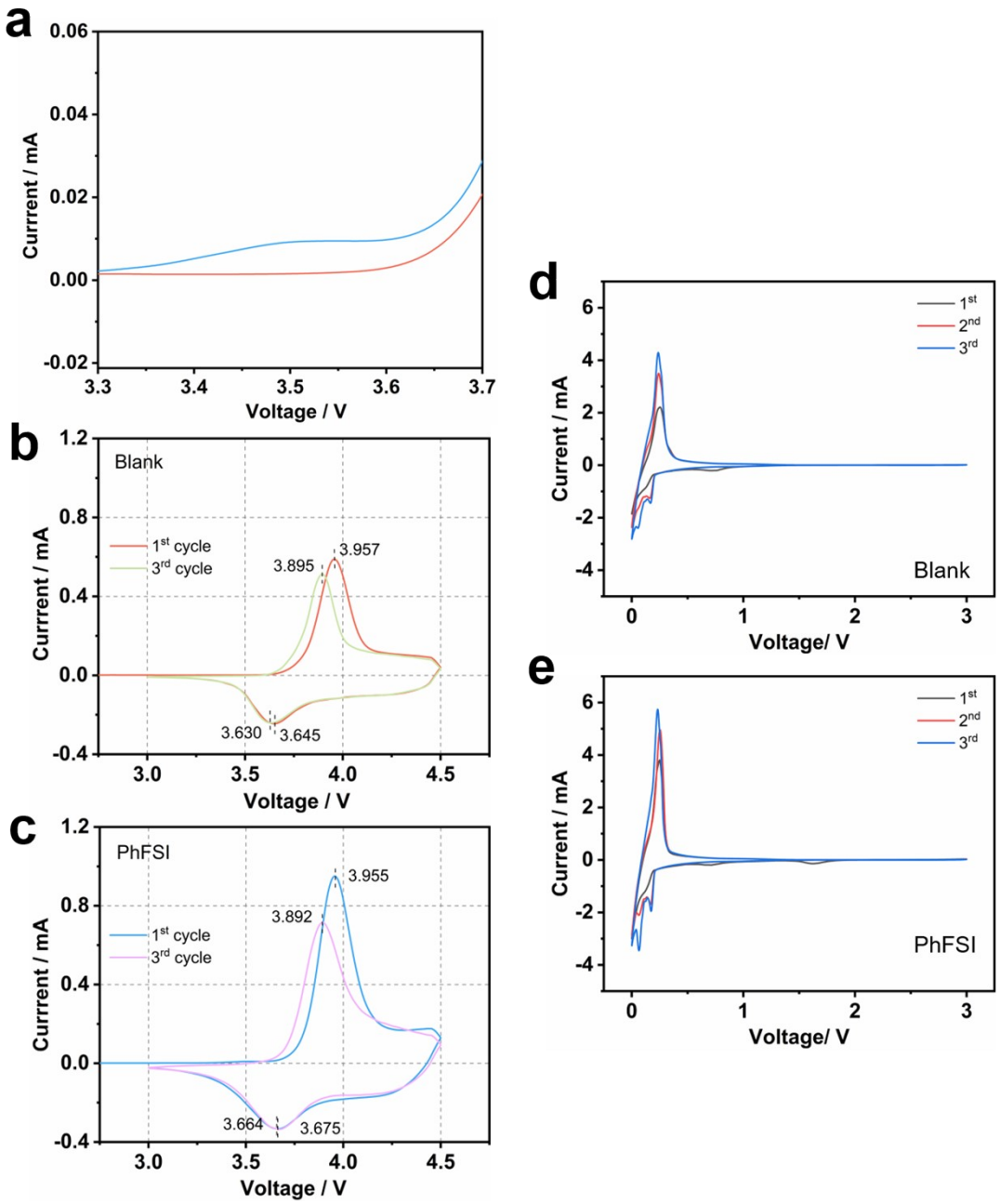

Fig. S11 (a) The magnified area and (b, c) 3 cycles scanning of the CV graph of the NCM523/Li. The 3 cycles scanning of the CV graphs of the Graphite/Li (d) without and (e) with PhFSI

LSV results of the electrolyte with/without PhFSI and their ^{19}F NMR analysis

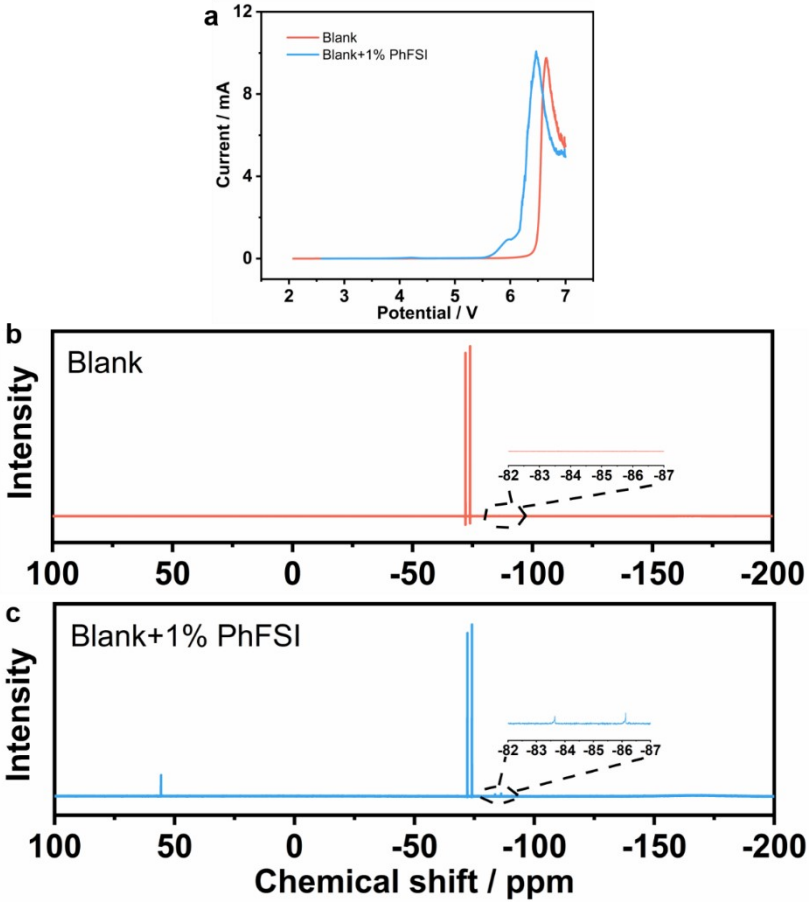

Fig. S12 (a) The LSV curves of the electrolyte with/without PhFSI scanned from OCV to 7 V. ^{19}F NMR results of the post-LSV electrolyte (b) with the Blank and (c) with the PhFSI..

Cycling performances of Graphite/Li with/without PhFSI

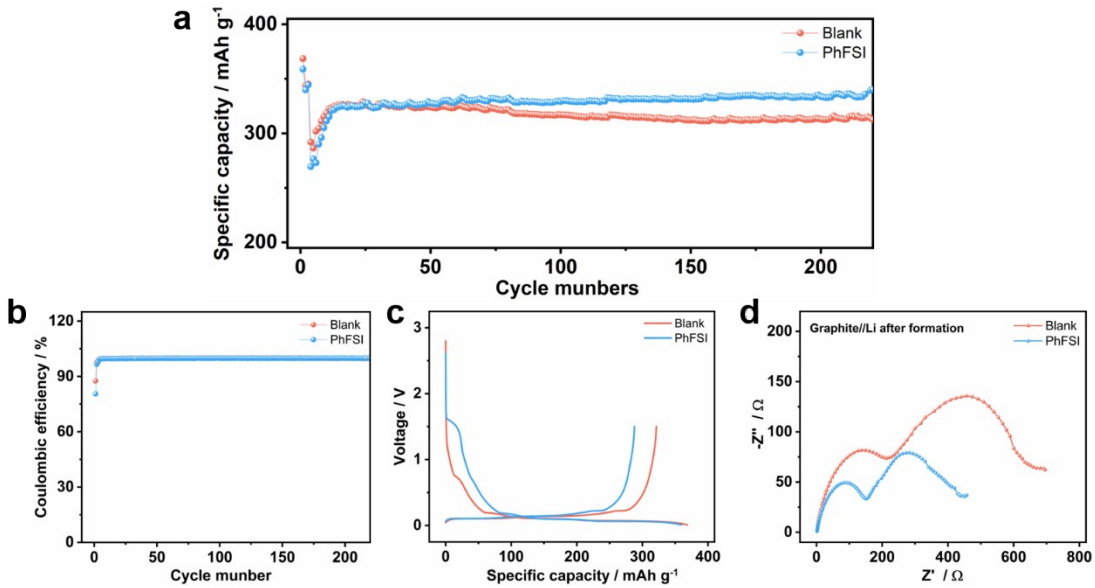

Fig. S13 (a) The cycling performance of the Graphite/Li with and without PhFSI started at 0.1 C (1C = 372 mAh/g) for 3 cycles with following cycling at 0.5 C at 25 °C. (b) The coulombic efficiencies during the cycling. (c) The initial charge-discharge curve at 0.1 C. (d) The EIS spectra of the Graphite/Li cells after formation of cycling at 0.1 C for 3 cycles.

The Possible electrochemical decomposition mechanism of PhFSI additive

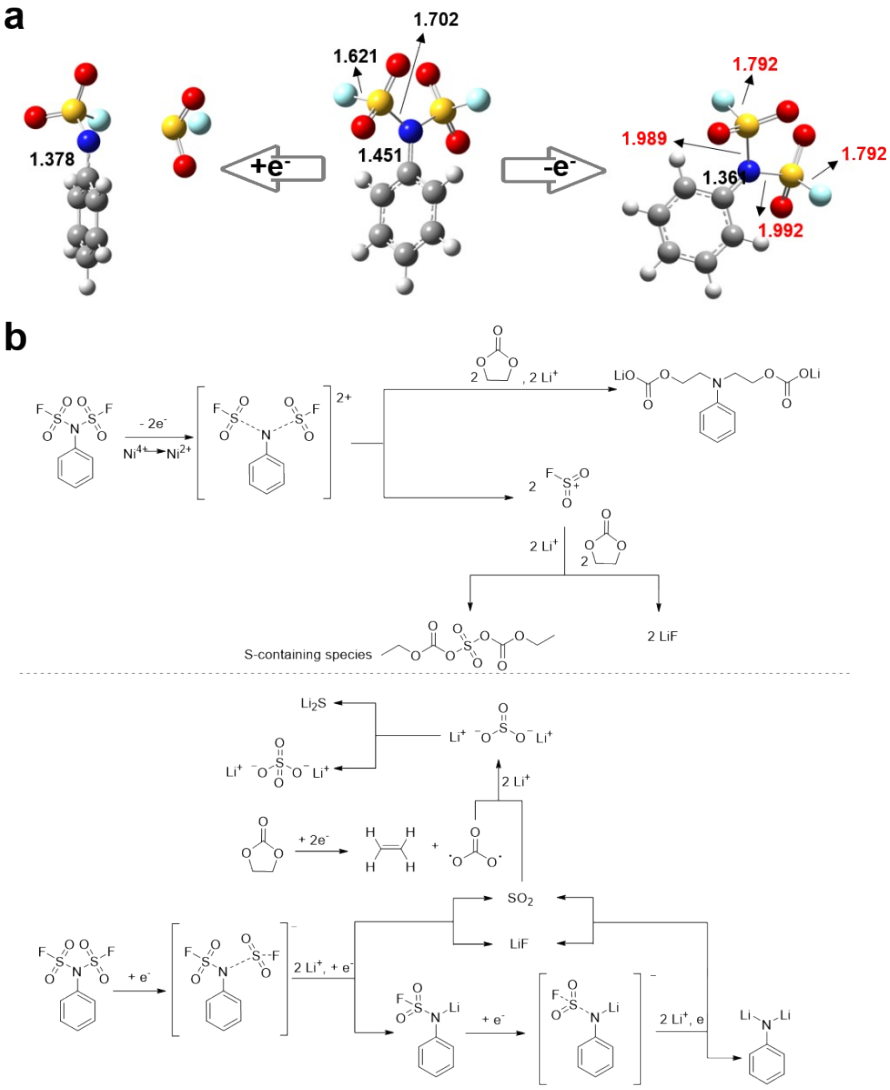

Fig. S14 (a) The optimized structures of the PhFSI with bond length at neutral state and after gaining/losing one electron. (b) The functional mechanism illustration of the PhFSI on the cathode and the anode.

To figure out the mechanism of PhFSI additive molecular, the structures of the PhFSI at neutral, after acquiring and losing one electron states were optimized though DFT calculations, as shown in Fig. S14. On the cathode, the oxidation is considered to start with the leaving of two -SO_2F groups after losing electrons, suggested by the longer S-N bond lengths in comparison with neutral state. When gaining one electron on the anode, only one -SO_2F group exhibits obvious leaving trend with one remaining on the additive molecule, which is supposed to leave in the following reduction process as well. The resultant -SO_2F group will further undergo reaction with EC and Li^+, and eventually generate the resultant LiF, Li sulfite/sulfate/sulfide. C-N bond lengths even shrink after PHFSI undergoes oxidation and reduction, which may attribute to the stabilization of the conjugation effect and explain the existence of species with C-N bond in Fig. 3. Based on the XPS as well as DFT calculations, the functional mechanism

of PhFSI was proposed in detail as shown in Fig. S14b.

Reference

1. T. Guo, G. Meng, X. Zhan, Q. Yang, T. Ma, L. Xu, K. B. Sharpless and J. Dong, *ngew. Chem. Int. Ed.*, 2018, **57**, 2605-2610.
2. H. Li, J. Cai, J. Liao, Y. Li, X. Zeng, X. He, W. Fan, C. Fan, Z. Ma and J. Nan, *JJ. Mater. Chem. A*, 2023, **11**, 24970-24981.